Highly durable amphiphobic coatings and surfaces: A comparative step-by-step exploration of the design variables

Magda Blosi, Federico Veronesi, Giulio Boveri, Guia Guarini, Mariarosa Raimondo

PII: S0257-8972(21)00593-4

DOI: https://doi.org/10.1016/j.surfcoat.2021.127419

Reference: SCT 127419

To appear in: *Surface & Coatings Technology*

Received date: 15 April 2021

Revised date: 9 June 2021

Accepted date: 10 June 2021

Please cite this article as: M. Blosi, F. Veronesi, G. Boveri, et al., Highly durable amphiphobic coatings and surfaces: A comparative step-by-step exploration of the design variables, *Surface & Coatings Technology* (2021), https://doi.org/10.1016/j.surfcoat.2021.127419

Covering Letter

Dear Editor,

please find enclosed the manuscript titled: *Highly durable amphiphobic coatings and surfaces: a comparative step-by-step exploration of the design variables* by Magda Blosi, Federico Veronesi, Giulio Boveri, Guia Guarini and myself for the publication in **Surface and Coatings Technology.**

The paper deals with the production of aluminum amphiphobic surfaces by deposition of organic inorganic hybrid thin coatings with different composition - designed by more traditional or SLIPS biomimetic approaches - on differently textured susbtrates.

The most innovative aspects of the paper, with respect to the previous state of the art too, lie in the step-by-step comparison adopted along the work that allowed the assessment of the relative incidence of the substrate/coating/processing variables to maximize both static and dynamic repellence against liquids. The following order was found: morphology of the inorganic layer (*flower*- or *spherical like*) > substrate roughness at microscale > nature of organic fluoropolymer.

Moreover, in the standview of the industrial application of Al with innovative functional surfaces, whose performances are linked in a complex way to the different variables, the paper provides criteria for the design of highly durable amphiphobic material suitable to be adopted under severe working environments.

Best regards

Mariarosa Raimondo
Corresponding author

ISTEC CNR
Faenza (Italy)
mariarosa.raimondo@istec.cnr.it

Highly durable amphiphobic coatings and surfaces: a comparative step-by-step exploration of the design variables

*Magda Blosi, Federico Veronesi, Giulio Boveri, Guia Guarini, and Mariarosa Raimondo**

CNR-ISTEC, National Research Council - Institute of Science and Technology for Ceramics, via Granarolo, 64 40018 Faenza (Italy)

*Corresponding author: mariarosa.raimondo@istec.cnr.it, ph. +39 0546 699721

Abstract

The design and production of amphiphobic surfaces with enhanced durability is increasingly considered a hot topic. It is well known that the material's repellence against liquids is regulated by morphological and chemical features of the working interfaces under different conditions. In this work the approach to the fabrication of highly repellent surfaces against both water and low surface tension oils is presented for a better understanding of the role played by different variables, e.g. the substrate surface finishing when multicomponent hybrid coatings with a different structural organization and chemistry are deposited. As suggested by biomimetic criteria, hierarchical features, when coupled with low surface energy moieties, are able to provide liquid repellence for different practical scopes. This work has been focused on coating processes applied to aluminum alloys with different surface roughness by deposition of nanostructured ceramic oxide (Al_2O_3, SiO_2 and TiO_2) and fluoro-polymers (fluoroalkylsilane or acrylic resin). It was found that the relevance of the substrate/coating variables involved in maximizing the static and dynamic liquid repellency follows the order: morphology of the inorganic layer > substrate roughness at microscale > nature of organic fluoropolymer. Both *flower-* and *spherical-like* inorganic nanostructures actually promote a significant improvement of the repellence with respect to the organic layer alone, with Al_2O_3 *flower-like* nanostructure being the most performant. Generally speaking, most hybrid-coated surfaces showed a good ability to withstand severe environments, the different response depending on the composition of the inorganic layers and not from the overall coating

morphology. The step-by-step comparison of results suggests that the perspective for the application of such a kind of surfaces is related in a complex way to textural and chemical variables influencing the final performances which could stay unchanged or vary depending on the exposure environment and conditions.

Keywords: amphiphobicity; hybrid coatings; static and dynamic wetting; abrasion resistance; chemical stability

1. Introduction

The control of surface wettability devoted to the achievement of hydrophobicity or oleophobicity has been of great interest to researchers in scientific and industrial field due to the strong demand for several applications such as self-cleaning [1,2], non-staining surfaces [3], spill-resistance [4], personal protection [5], drag reduction [6], corrosion prevention [7,8], anti-icing [9,10], anti-biofouling [11–13], liquid separation [14,15], protection of buildings [16,17], functionalization of textiles [18] etc. For the majority of these applications, amphiphobic or superamphiphobic surfaces, i.e. being hydrophobic and oleophobic at the same time, are much more desirable than those having repellence or even super-repellence only to either water or oil. Generally, a superamphiphobic surface shows extraordinary non-wetting properties due to the simultaneous existence of specific topographical patterns (micro-nano roughness) and low surface energy [19,20].

Several methods have been developed to fabricate amphiphobic or superamphiphobic surfaces by means of multistep approaches. For examples, two-step processes including roughening surfaces using nanoparticles (NPs) [3,21–23], etching [24–27], lithography [28], template-assisted deposition [1], sputter coating [29], or sol–gel route [30], and subsequent treatments to lower surface energy have been reported. Among these techniques, wet chemical processes like dip or spray coating are of particular interest owing to their great versatility coupled with the convenience for large-scale manufacturing thanks to low reliance on equipment. In fact, in the literature the typical issues for an easy scale-up of the processes are often neglected, but the selection of easily scalable processing routes resents a fundamental requirement for the development of the technology in the real world.

Here, we present a widespread comparative study among twenty different surfaces prepared by a simple wet chemical coating method on aluminum supports, either rough or smooth. Basically, we developed hybrid coatings specifically designed by coupling an inorganic phase - in form of nanosol coming from a patented process developed in our laboratories [30,31] or

re-formulated by commercially available precursors - with an organic fluorine-bearing polymer.

The influence of both surface chemistry and morphology was systematically investigated aiming at a deeper understanding of the wetting phenomena. Specifically, we focused our attention on aluminum alloys surfaces coated by nanostructured hybrid layers, whose static (contact angles against water and n-hexadecane) and dynamic (contact angle hysteresis CAH calculated as the difference between advancing and receding contact angle) wetting behavior was studied.

The obtained results allowed to evaluate the strengths/weaknesses for each coating formulation. We systematically changed material variables - substrate roughness, coating morphology, inorganic layer composition (Al_2O_3, TiO_2 or SiO_2 nanoparticles in different media) and organic fluoro-polymer typology (fluoroalkylsilane FAS or fluorinated acrylic resin AFW) - investigating their influence on liquid repellence performances and durability.

2. Materials and methods

2.1 *Preparation of colloidal suspensions*

As reported in the literature, nanoparticles concentration of the suspension could affect the final wetting performance of the surfaces [32]. However, here the nanoparticles concentration was not investigated as relevant variable, because all the procedures presented to prepare the nanosuspensions represent the optimized ones in term of synthesis process and nanoparticles concentration. Alumina nanoparticles in form of alcohol- and water-based suspensions were prepared following our patented procedure [30,31].

Al_2O_3 alcohol-based sol (Al(ipa)) 25.39 g of aluminum-tri-sec-butoxide (97%, Sigma–Aldrich) were added to 146.18 ml of isopropyl alcohol (Sigma–Aldrich 99.7%) and kept under stirring for 1 hour within a chamber at room temperature and controlled humidity (5%). Then 12.88 ml of the chelating agent, ethyl acetoacetate (>99%, Sigma–Aldrich) were added

and after 3 hours a mixture of 7.21 ml of water with 7.21 ml of isopropyl alcohol was added dropwise and stirred for 24 hours at room temperature. The final Al_2O_3 concentration in the sol was 5%wt.

Al_2O_3 water-based sol (Al(w)) 22.26 ml of ethyl acetoacetate, as chelating agent, were added to 158.72 ml of deionized water and mixed for few minutes and gently heated. Once temperature reached 70°C, 44.69 g of aluminum-tri-sec-butoxide and 123.48 ml of nitric acid aqueous solution (0.5 M) were added to promote peptization. The reaction mixture was left under stirring at 70°C for 24 h. The molar ratios of chelating agent, nitric acid and total water with respect to the metal alkoxide were set to 1, 0.3 and 90, respectively. The resulting pH of the as-prepared sol was 3.6 and the Al_2O_3 concentration of 5%wt.

SiO_2 water-based sol (Si) The adopted SiO_2 coating material was a stable suspension (Ludox HS40, 40%wt, Grace Davidson), with an average particle diameter of 20 nm that, before the deposition on the substrate, was diluted till a concentration of 4%wt.

TiO_2 water-based sol (Ti). The adopted TiO_2 coating material was a stable suspension (Parnasos, PH000026 Colorobbia Italia, 6%wt) with an average particle diameter of 15 nm that, before deposition, was diluted till a concentration of 3%wt.

2.2 *Characterization of colloidal suspensions*

Particle size distribution and average hydrodynamic diameter of Al_2O_3, SiO_2 and TiO_2 suspensions were measured by a dynamic light scattering analyzer (DLS, Zetasizer Nano S, Malvern Instrument) working at 25°C in backscattering mode (detection angle 173°). Hydrodynamic diameter includes the coordination sphere and the species adsorbed on the particle surface such as stabilizers, surfactants, and so forth. DLS analysis also provides a polydispersity index (PDI), whose value, ranging from 0 to 1, is related to the dispersion degree of colloidal suspension. The suspensions here prepared showed different hydrodynamic diameters. DLS of water-based Al_2O_3 showed a single peak with an average

particle size centered at 44 nm, while the alcohol-based one showed a multimodal particle size distribution, the peak with the highest scattering intensity being centered at 4 nm with smaller amounts of aggregate particles (Supporting Information Fig. S1).

2.3 Deposition of hybrid coatings

After ultrasonication in ethanol for 5 min to remove impurities, aluminum alloy (Al1050 99% H24) foils, with dimensions of about 100 x 50 x 1.5 mm, have been systematically coated by dip-coating in the different inorganic sols. Aluminum foils with two different surface textures were considered. The smooth samples (S series) were used as received and showed an average roughness R_a of about 0.5 µm as evaluated by Contour GT-K Bruker GmbH optical profilometer, while the sandblasted rough ones (obtained with Swarco corundum sand, 400-800 µm grit, R series) showed average R_a values of about 4.5 µm. Basically, the developed approach implied the deposition of the inorganic layer first, followed by the grafting of fluorinated molecules. S and R samples only bearing organic layers have also been produced as reference (Table I). Depending on the kind of the inorganic coating, different processing routes were pursued, as schematized in Figure 1.

Al_2O_3-based coatings with flower-like morphology (Al(ipa) and Al(w) sample series). The deposition of Al_2O_3 nanoparticles, suspended in isopropyl alcohol or water, is a multistep procedure requiring different annealing steps together with an intermediate boiling treatment to promote the transformation into boehmite of the inorganic layer and the nanostructuring as well [33]. Al alloy foils were dip-coated into the Al_2O_3 sols under the following conditions: dipping/withdrawing speed of 2 mm/s and soaking time of 5 s. After drying at room temperature, coated samples were treated at 400°C for 60 min, then boiled in distilled water for 30 min to form flower-like nanostructured bohemite AlOOH, and thermally treated again at 400°C for 10 min. Finally, two different, cost-effective fluorine-bearing polymers easily available on the market, were selected: a fluoroalkylsilane dispersed in isopropyl alcohol

(Dynasylan SIVO CLEAR EC, Evonik) and a fluorinated acrylic resin dispersed in water (AFW 730. Chem Spec). Such polymers were dip-coated on the inorganic underlayers (dipping/withdrawing speed: 2 mm/s, soaking time: 120 s), then annealed at 150°C for 30 min [34].

SiO_2 and TiO_2-based coatings with spherical-like morphology (Si and Ti sample series). The processing of SiO_2 and TiO_2 coatings does not require the boiling step (Figure 1) involving the inorganic layer deposition (dipping/withdrawing speed: 2 mm/s, soaking time: 5s) followed by heat treatment (400°C for 60 min), deposition of either SIVO or AFW (dipping/withdrawing speed: 2 mm/s, soaking time: 120 s) and subsequent consolidation in oven (150°C for 30 min). The details of coatings composition are summarized in Table I while the schematic representation of multilayered coated samples is given in Figure 2.

2.4 *Characterization of coated surfaces*

The wetting properties of coated and uncoated surfaces taken as benchmark were determined through the measurement of contact angles with an optical contact angle system (DSA 30S, Krüss GmbH). In static contact angle measurements, 10 µL drops of the test liquid (either deionized water or n-hexadecane from Sigma-Aldrich) were dispensed by a software-controlled syringe and deposited on the surface. Every surface was investigated with 3 to 10 drops per liquid and average contact angle against water (WCA) and hexadecane (CA-Hex) were computed.

Advancing and receding contact angles with water and hexadecane drops were measured for all surfaces in order to calculate the contact angle hysteresis (CAH) which is related to their dynamic wetting behavior, i.e. the smaller the hysteresis, the higher the water drop mobility. For these measurements, a 10 µL water drop was dispensed by a syringe and slowly put in contact with the surface. Then, 5 µL of water were added and the advancing contact angle (ACA) was measured as the drop-surface contact point moved outward. Further, water was withdrawn from the drop and the receding contact angle (RCA) was measured as the contact

point moved inward. CAH was calculated as the difference between ACA and RCA in one point. Three to five measurements were performed for each sample.

The surface morphology of coated samples was investigated with a field-emission scanning electron microscope (FE-SEM Gemini Columns SIGMA Zeiss).

2.5 *Durability tests*

In order to verify the tribological and chemical resistance of coated surfaces, different durability tests were performed. For this purpose, samples underwent abrasion test, acid, alkali, salt, marine water attacks and UV irradiation, then their behavior was compared with that of the uncoated ones monitoring WCA, CA-Hex and CAH over the time. For the acidic environment, a solution of acetic acid (pH 3) was prepared, while for the alkaline test a NaOH solution (pH 12) was used. The resistance towards salts was assessed by soaking the samples into a highly concentrated NaCl solution (100 g/L) for a total time of 14 days. In order to monitor the surface degradation, samples were periodically withdrawn from the test solutions, rinsed with distilled water, air-dried and subjected to the measurements of contact angles. After that, they were immersed again in the test solution. The resistance toward UV radiation was assessed by keeping the samples under an UV lamp (Ultravitalux 300 W, OSRAM) for 8 hours with an irradiation power of 10 mW/cm^2 (measured at the surface) at λ = 354 nm. Abrasion tests were performed according to the UNI EN 1096-2 standard [35]. A felt disk (diameter 4 cm) was pressed against the surface applying a normal force of 4 N, then it started rotating with a speed of 60 rpm for 30 seconds.

3. Results and discussion

3.1 The role of the organic fluoropolymer

As known by the literature, the surface chemical composition plays a key role in materials wettability as it determines their surface energy and their attitude to interact with the

surrounding environment. To accomplish hydrophobicity or oleophobicity on a flat solid surface, i.e. a contact angle higher than 90° for water or oil droplets, Young's theory [36] suggests that surface free energy should be smaller than one quarter of that of the liquid [37] to be repelled. Dealing with low surface tension oils, this can be achieved when molecular groups like $-CF_3$ and $–CF_2–$ are grafted to the surface.

For a better understanding of the role played by each component of the hybrid coating (Figure 2), substrates only coated with the organic polymers were prepared as a first step. Here, the effects of substrate texture (smooth or rough) and of different applied polymers (SIVO or AFW) are well detected without the interaction of the oxide layer. A clear hydrophobic behavior was well appreciated for all the samples, neither reaching the superhydrophobic regime nor showing oleophobicity (Table II).

As expected, some differences were detected among samples. WCA and CA-Hex are markedly increased for the rough surfaces promoting a general improvement of the liquid repellency. Conversely, with the same surface finishing, no relevant differences were detected by comparing SIVO and AFW fluoropolymers so further emphasizing the role of the roughness on the static wettability when coupled with a specific surface chemistry, as consistent with the Wenzel wetting model [37].

In any cases, the polymeric coating alone, without any underlying structure at the nanoscale, did not promote a satisfactory water droplet mobility with CAH values higher than 70°. That said, it was observed a more positive effect of surface smoothness on drop mobility (Table II), due to a lower amount of pinning points during the droplets motion.

Furthermore, we did not report details for samples coated by the inorganic layer only, because they all exhibited superhydrophilic behaviors with WCA values lower than 10° as consistent with the presence of nanostructured oxides, but not relevant in a surface design perspective for amphiphobic purposes.

3.2 Structure of the hybrid coatings

As expected, the presence of the nanostructured inorganic underlayer enabled the improvement of the surface liquid repellence. As proved by FESEM images (Figure 3), two different kinds of nanostructures were achieved by means of the processes outlined in Figure1: *flower-* and *spherical-like* detected, respectively, for the Al_2O_3 (Figure 3a, b) and SiO_2, TiO_2-based coatings (Figure 3c, d). Al_2O_3-based coatings in both water and alcohol medium produced the same typical *flower-like* morphology, with a slightly finer and more packed nanostructure associated to the alcoholic suspension (Figure 3b). Despite several studies report a correlation between particle size and hydrophobicity of the coating [38,39], for such Al_2O_3-based coatings this effect is really mitigated, because nanoparticles are not directly responsible for the formed nanostructure as they undergo a strong physicochemical transformation into boehmite lamellae during the boiling step, therefore the influence of the starting nanoparticle size assessed in suspension (see Figure S1_Supporting information) cannot be directly linked to the final performance. We observed that depending on the dispersion medium, the length of lamellae was different with average values of about 100-150 nm and 200 nm, respectively, for alcohol- and water-dispersed nanoparticles, probably due to a different physicochemical response of the two xerogel films deposited on the surfaces to the boiling water treatment.

SiO_2 and TiO_2 produced very similar morphologies as well, associated to a homogenous nano-spherical layer spread on the treated surface and evidencing at higher magnification the presence of the primary nanoparticles.

3.3 Static repellence

The data collected in Table III provide relevant differences based on the kind of surface nanostructure with the repellence attitude of *flower-like* morphologies standing out with respect to the *spherical-like* ones. Al_2O_3-based coatings presented the best performance with

WCAs in the 141-167° range, while SiO_2- and TiO_2- based ones evidenced WCAs in the 113-135° range, these latter values being similar to those provided by the organic layers alone (Table II). Probably, the lamellar morphology typical of *flower-like* alumina allows to reach the Cassie-Baxter wetting state, thanks to the complex nano-voids system with entrapment of an air layer. No relevant differences in terms of WCA were ascribed to the *flower-like* structures provided, respectively, by water-and alcohol-based alumina.

CA-Hex values, ranging from 97° to 121°, confirmed the better performance of the *flower-like* nanostructure. On the other hand, the *spherical-like* coatings exhibited CA-Hex values in the 70-83° range, below the oleophobic threshold but improved with respect to the uncoated aluminum (CA-Hex of 19°) and a little bit higher than those provided by the organic coating alone (CA-Hex between 65 and 74° in Table II). Generally speaking, these results pointed out that both *flower-* and *spherical-like* inorganic nanostructures actually promote a significant improvement of the repellence with respect to the organic layer alone, this circumstance strengthening their role into the design of multilayered highly repellent coatings.

Besides the nanostructure morphology, the second relevant variable influencing the final performance resulted to be the roughness of the aluminum supports. In most cases, for the same coating composition, the transition from a rough to a smooth support led to a significant reduction of both WCA and CA-Hex. As known in the literature [40–42], the dual-scale texture typical of a hierarchical organization can help to increase the stability of the Cassie-Baxter wetting state when repellence against water is concerned.

3.4 Dynamic repellence

The same considerations pointed out in Section 3.3 on the key surface parameters influencing the static behavior appear to be valid for the dynamic repellency as well. Water CAH values highlighted again the heavy influence of the nanostructure, followed by the effect induced by the surface roughness and, in last place, by the kind of organic polymer. Particularly, the

flower-like samples (Al(ipa) and Al(w)) well support the self-cleaning behavior and confirm the improved performances for the rough substrates. Since the Cassie-Baxter state is stabilized by the hierarchical dual scale texture, a depletion of mobility was observed passing from rough to smooth substrates. The best dynamic results were ascribed to Al(ipa) and Al(w) samples, with SIVO as organic polymer, which showed water CAH as low as 3-4° for the rough surfaces and 5 to 8° for the smooth ones.

A significant worsening occurred when AFW was selected as organic component. In fact, water CAH values increased from about 16° for the rough support up to 146° for the smooth ones. Here, the small receding contact angles (RCA) point out a poor de-wetting ability due to strong sticking phenomena.

Such a different dynamic performance of the organic polymers stems from their different chemical nature: SIVO product is classified as a fluoroalkylsilane polymer provided in isopropyl alcohol solution, while AFW belongs to the fluorinated acrylate resin class in form of water-based solution. Although their actual structural formulas were not disclosed by the producer, FT-IR analyses (See Figure S2_Supporting information) highlighted a stronger contribution of the C-F bonds for the SIVO polymer, which probably is the reason of its better amphiphobic performance. Moreover, AFW is a water-based product and it may have generated inhomogeneous layers on the smooth substrates due to poor wetting, while the alcohol-based SIVO forms a homogeneous layer on boehmite [43].

As expected, the *spherical-like* nanostructure, associated to a Wenzel regime, evidenced a drastically different dynamic behavior. The high water CAHs, from 52 to 129°, imply marked pinning phenomena for all the samples, however the data analysis revealed some differences among the surfaces. The droplet mobility increased for the smooth surfaces which offer fewer pinning points, as verified for the organic coating alone. In addition, the recorded water CAH compared with those of the organic layer alone showed that SiO_2 coating coupled with SIVO is the only solution able to enhance the drop mobility with respect to the polymer alone.

Summarizing, some common trends can be drawn with regards to the influence of the different variables on products wettability (Figure 4). The main role in determining the wetting properties is played by the kind of nanostructure, with *flower-like* morphology being the most performant in terms of both static repellence and dynamic droplet mobility. The second more influent feature is the texture at the microscale, implying in most cases increased results for the sandblasted rough surfaces. Finally, the least influent parameter is the organic layer type, with the fluoroalkylsilane promoting an enhanced behavior in terms of liquid repellence.

Hexadecane CAH was also measured for all surfaces, as reported in Table S1. Contrary to what observed with water drops, all coatings displayed poor dynamic repellence towards hexadecane drops due to its low surface tension, which caused penetration of the liquid between surface features and led to low RCA. Thus, hexadecane CAH was not considered for the following durability tests as it did not provide useful insight in the behavior of different coating formulations.

3.5 Wetting after abrasion

Generally speaking, most of the coated samples showed a good abrasion resistance (the results are fully reported in Table S2 of Supporting Information). The graphs displayed by Figures 5 and 6 show the wetting properties of, respectively, *flower-like* and *spherical-like* coated samples after abrasion, whose analysis can been undertaken looking at the different variables - surface texture, inorganic layer structure and composition, kind of organic layer, etc. - involved time by time. Despite the tribological action affected in some way the conservation of alumina nanostructure with an overall depletion of liquid repellence, the *flower-like* samples preserved a satisfactory hydrophobicity with WCA higher than 130° and even higher than 140° when rough surfaces were coupled with SIVO (Figures 5a and 6a). Furthermore, no influence was played by the different suspension medium (isopropyl alcohol

or water). As far as the organic layer typology, the AFW polymer confirmed to be less effective than SIVO in keeping the wetting unchanged, mainly when droplet mobility is concerned. From the droplet mobility perspective, the scenario appeared changed: the *flower-like* nanostructured coatings revealed a marked increase in CAH causing a sticking behavior of the surfaces. This is the consequence of the mechanical stress partially affecting the surface homogeneity, to whom CAH is strictly linked (Figures 5 and 6). The micrographs evidenced the presence of some damaged areas characterized by a flattened flower-like nanostructure. As a result, CAH jumped from 4-10° to 40°-70° after abrasion, accompanied by the abrupt decrease of the receding angles, clear expression of the increased de-wetting difficulty. On the contrary, no differences were appreciated before and after abrasion on the *spherical-like* nanostructures for both rough and smooth surfaces. Similarly, the oleophobicity after abrasion was depleted, but eventually preserved, with CA-Hex ranging from 93 to about 125°. Notwithstanding the influence of the different variables on CA-Hex is quite complex, AFW seems to be more effective than SIVO in preserving the repellence against oil after abrasion. Figure 7 shows the percentage variations of WCA, CAH and CA-Hex calculated with respect to their starting values. The data were here gathered into two main groups: *flower-like* and *spherical-like* coatings, disregarding the variations of surface texture and organic layer. This way, the data revealed the overall difference, highlighting a better abrasion resistance of the *spherical-like* coatings although they clearly showed poorer performances with respect to the *flower-like* ones.

After abrasion, FESEM micrographs evidenced the presence of some damaged areas on the Al based coating (Figure 8a) characterized by the flattening of *flower-like* nanostructure as pointed out at higher magnification (Figure 8b). As a result, CAH jumped from 4°-10° to 40°-120° after the test, accompanied by the abrupt decrease of the receding angles (RCA), clear expression of the increased de-wetting difficulty.

SiO_2 coating, considered as benchmark for the *spherical-like* nanostructure, highlighted some abrasion tracks (Figure 8c), however at higher magnification an almost regular nanostructure was observed (Figure 8d), as consistent with the slight variations assessed for the CAH values of this kind of surface.

3.6 Resistance to UV irradiation

In view of the potential application of low-wettable materials in outdoor environments, the resistance under UV irradiation of the coated surfaces was investigated. The UV resistance is defined as the ability of a material to withstand ultra-violet radiation or sunlight which could promote an extensive weathering of their surface performances. Due to their hybrid nature, the amphiphobic coatings investigated in the present work could be potentially affected by UV radiation with the formation of hydrophilic groups leading to detrimental oxidation effects on the outer polymeric layers. However, the results here collected (Table S3 in Supporting Information) pointed out the very good stability of all samples even after 8 hours of direct UV irradiation with both static and dynamic wettability that stayed practically unchanged after the exposure. Although TiO_2 coating could trigger a photodegradation reaction, no alterations were observed for this material which presents a citrate shell around the nanoparticles able to mitigate its photoreactivity [44]. Only for Al_2O_3_AFW coatings we observed some WCA variations that were always able to keep the static contact angles higher than 140°.

3.7 Chemical durability

Chemical durability represents another key issue to evaluate the potentiality of functional surfaces in extreme, harsh environments. In this paper the amphiphobic surfaces were kept in highly saline water and corrosive liquids (acids and bases) for exposure times up to 14 days, several orders of magnitude longer than the common tests presented in the literature generally referring to contact time with corrosive liquids from 50 minutes [45] to 24 hours [46]. Figure

9 shows the WCA evolution after 14 days soaking of Al_2O_3(ipa) and SiO_2- based coatings as representative of flower and spherical-like nanostructures respectively. Chemical durability for Al_2O_3(w), and TiO_2 coatings are reported in Figure S4 (Supplementary information).

The results highlighted a relevant role played by the different kind of organic polymer. In fact, for both the *flower*- and *spherical-like* nanostructures the AFW polymer is more sensitive to the hydrolysis induced by corrosive solutions, while SIVO evidenced a stronger protective action against all the environments. The fluoroalkylsilane polymer is probably more stable thanks to the SiM-O-metal bonds established with the hydroxyl groups of the inorganic layer and further stabilized by the cross-linking bonding among free Si-OH groups, generated by the FAS hydrolysis under environmental humidity [42].

In addition, Figure 9 highlights that the WCA decreasing in presence of AFW was already detectable after 3 days soaking with a progressive worsening occurring over the following days. According to the different inorganic layers, the Al_2O_3_AFW samples exhibited the worst durability when soaked into saline and basic solutions, with a WCA depletion of, respectively, 35-40% and 40-50%, while the SiO_2 AFW sample evidenced the poorest resistance into the acidic environment, with a WCA depletion of about 50%.

The different response to the environments stems from the different composition of the inorganic layers and not from their different morphology. Once the AFW is hydrolyzed and the corrosive solutions come in contact with the inorganic layer, the different chemistries drive the corrosion process as already found in our previous paper [33]. Both Al_2O_3 based coatings pointed out very close data each other's, it can be hypothesized that the aluminum oxide layer reacts with alkaline compounds forming aluminum oxide anions (AlO_2^-) which turn into aluminum hydroxide ($Al(OH)_3$) triggering a series of equilibrium reactions able to induce the progressive damage of the inorganic substrate. On the other hands, SiO_2 (applied in form of nanosol stabilized at basic pH - could be mainly affected by an external acidic environment.

The smooth supports confirmed a more marked decreasing of performance due to the lower grafting degree of the AFW polymer on such flat surfaces. On the opposite, SIVO polymer always ensured an outstanding protection against all the corrosive environments, with the rough textures showing the highest durability under these conditions, with a lowering of WCA as low as 10% during the 14 days. A similar trend was observed for CA-Hex values (Figure S5_Supporting Information).

4. Conclusions

This work refers to the design and characterization of Al_2O_3-, SiO_2- and TiO_2-based amphiphobic hybrid coatings after deposition on rough or smooth aluminum substrates. The comparative step by step investigation here presented sheds light on the relationships among the different substrate and coatings features - e.g. the substrate surface finishing when multicomponent hybrid coatings with a different structural organization and chemistry are deposited - and their role on wetting performances and lasting behavior of coated surfaces. Generally speaking, the relative incidence of the different parameters in maximizing the static and dynamic repellence against liquids (both water and n-hexadecane) follows the order: morphology of the inorganic layer > substrate roughness at microscale > kind of organic fluoropolymer. The main role in determining the wetting properties of hybrid coatings is played by the morphology of the inorganic component. As far as the morphology of the inorganic component, the Al_2O_3 *flower-like* nanostructure revealed to be the most performing in terms of both static repellence and dynamic droplet mobility. As already reported in the literature [40–42], the dual-scale texture typical of a hierarchical organization - as the result of the proper combination between the substrate micro-roughness and inorganic layer nanostructure - promotes the stability of the Cassie-Baxter wetting state thanks to the complex nano-voids system with entrapment of air layers. Finally, the least influent parameter is the organic layer type, with the fluoroalkylsilane promoting a greater amphiphobicity and lower hysteresis with respect to the acrylic resin.

Different ageing tests allowed to assess the greater or lesser ability of such hybrid coated surfaces to withstand severe environments. Abrasion tests on *flower-like* alumina-based coatings promoted flattening of the nanostructure accompanied by the abrupt decrease of de-wetting abilities. Indeed, a better abrasion resistance of the *spherical-like* coatings was highlighted. All coated samples showed a good stability under UV irradiation even for prolonged exposure time. As far as the chemical resistance, indeed, the role of the organic polymer stands out regardless of *flower-* or *spherical-like* nanostructures with fluorine bearing acrylic resin being more sensitive to the hydrolysis induced by corrosive solutions. For the same organic layer, Al_2O_3-based samples exhibited the worst durability when soaked into saline and basic solutions while SiO_2- and TiO_2-based ones evidenced the lowest resistance into the acidic environment. The smooth samples confirmed a more marked decreasing of performances due to the lower grafting degree of the acrylic fluoropolymer on such flat surfaces. On the opposite, fluoroalkylsilane ensured an outstanding protection against all the corrosive environments, with the rough textures showing the highest durability under these conditions.

Overall, from the perspective of their potential application under severe real conditions and mechanical stresses, it can be said that the design of such kind of surfaces requires a strict control of different parameters which are related to each other in a rather complex way.

List of references

[1] X. Deng, L. Mammen, H.-J. Butt, D. Vollmer, Candle soot as a template for a transparent robust superamphiphobic coating, Science. 335 (2012) 67–70. https://doi.org/10.1126/science.1207115.

[2] T. Sun, L. Feng, X. Gao, L. Jiang, Bioinspired Surfaces with Special Wettability, Acc. Chem. Res. 38 (2005) 644–652. https://doi.org/10.1021/ar040224c.

[3] B. Leng, Z. Shao, G. de With, W. Ming, Superoleophobic Cotton Textiles, Langmuir. 25 (2009) 2456–2460. https://doi.org/10.1021/la8031144.

[4] J.S. Bois, F. Jülicher, S.W. Grill, Pattern Formation in Active Fluids, Phys. Rev. Lett. 106 (2011) 028103. https://doi.org/10.1103/PhysRevLett.106.028103.

[5] S. Pan, A.K. Kota, J.M. Mabry, A. Tuteja, Superomniphobic Surfaces for Effective Chemical Shielding, J. Am. Chem. Soc. 2 (2013) 1–10. https://doi.org/https://doi.org/10.1021/ja310517s.

[6] X. Zhang, J. Zhao, Q. Zhu, N. Chen, M. Zhang, Q. Pan, Bioinspired Aquatic Microrobot Capable of Walking on Water Surface Like a Water Strider, ACS Appl. Mater. Interfaces. 3 (2011) 2630–2636. https://doi.org/10.1021/am200382g.

[7] H. Jin, M. Kettunen, A. Laiho, H. Pynnë, J. Paltakari, A. Marmur, O. Ikkala, R.H.A. Ras, Superhydrophobic and Superoleophobic Nanocellulose Aerogel Membranes as Bioinspired Cargo Carriers on Water and Oil, Langmuir. 27 (2011) 1930–1934. https://doi.org/10.1021/la103877r.

[8] X. Yin, P. Mu, Q. Wang, J. Li, Superhydrophobic ZIF-8-Based Dual-Layer Coating for Enhanced Corrosion Protection of Mg Alloy, ACS Appl. Mater. Interfaces. 12 (2020) 35453–35463. https://doi.org/10.1021/acsami.0c09497.

[9] C. Wei, B. Jin, Q. Zhang, X. Zhan, F. Chen, Anti-icing performance of super-wetting surfaces from icing-resistance to ice-phobic aspects: Robust hydrophobic or slippery surfaces, J. Alloys Compd. 765 (2018) 721–730. https://doi.org/10.1016/j.jallcom.2018.06.041.

[10] G. Boveri, A. Corozzi, F. Veronesi, M. Raimondo, Different Approaches to Low-Wettable Materials for Freezing Environments: Design, Performance and Durability, Coatings. 11 (2021) 77. https://doi.org/https://doi.org/10.3390/coatings11010077.

[11] J. Genzer, K. Efimenko, Recent developments in superhydrophobic surfaces and their relevance to marine fouling: A review, Biofouling. 22 (2006) 339–360. https://doi.org/10.1080/08927010600980223.

[12] X.-M. Li, D. Reinhoudt, M. Crego-Calama, What do we need for a superhydrophobic surface? A review on the recent progress in the preparation of superhydrophobic surfaces, Chem. Soc. Rev. 36 (2007) 1350–1368. https://doi.org/10.1039/b602486f.

[13] Y. Long, X. Yin, P. Mu, Q. Wang, J. Hu, J. Li, Slippery liquid-infused porous surface (SLIPS) with superior liquid repellency, anti-corrosion, anti-icing and intensified durability for protecting substrates, Chem. Eng. J. 401 (2020) 126137. https://doi.org/10.1016/j.cej.2020.126137.

[14] G. Kwon, A.K. Kota, Y. Li, A. Sohani, J.M. Mabry, A. Tuteja, On-demand separation of oil-water mixtures, Adv. Mater. 24 (2012) 3666–3671. https://doi.org/10.1002/adma.201201364.

[15] M. Wu, G. Shi, W. Liu, Y. Long, P. Mu, J. Li, A Universal Strategy for the Preparation of Dual Superlyophobic Surfaces in Oil-Water Systems, ACS Appl. Mater. Interfaces. 13 (2021) 14759–14767. https://doi.org/10.1021/acsami.1c02187.

[16] D. Aslanidou, I. Karapanagiotis, D. Lampakis, Waterborne superhydrophobic and superoleophobic coatings for the protection of marble and sandstone, Materials. 11 (2018) 585. https://doi.org/10.3390/ma11040585.

[17] D. Aslanidou, I. Karapanagiotis, C. Panayiotou, Tuning the wetting properties of siloxane-nanoparticle coatings to induce superhydrophobicity and superoleophobicity for stone protection, Mater. Des. 108 (2016) 736–744. https://doi.org/10.1016/j.matdes.2016.07.014.

[18] D. Aslanidou, I. Karapanagiotis, Superhydrophobic, superoleophobic and antimicrobial coatings for the protection of silk textiles, Coatings. 8 (2018) 101. https://doi.org/10.3390/coatings8030101.

[19] B. Bhushan, Y.C. Jung, Natural and biomimetic artificial surfaces for superhydrophobicity, self-cleaning, low adhesion, and drag reduction, Prog. Mater. Sci. 56 (2011) 1–108. https://doi.org/10.1016/j.pmatsci.2010.04.003.

[20] A.R. Parker, C.R. Lawrence, Water capture by a desert beetle, Nature. 414 (2001) 33–34. https://doi.org/10.1038/35102108.

[21] C. te Hsieh, F.L. Wu, W.Y. Chen, Superhydrophobicity and superoleophobicity from hierarchical silica sphere stacking layers, Mater. Chem. Phys. 121 (2010) 14–21. https://doi.org/10.1016/j.matchemphys.2009.12.031.

[22] Z. He, M. Ma, X. Lan, F. Chen, K. Wang, H. Deng, Q. Zhang, Q. Fu, Fabrication of a transparent superamphiphobic coating with improved stability, Soft Matter. 7 (2011) 6435–6443. https://doi.org/10.1039/c1sm05574g.

[23] H. Zhou, H. Wang, H. Niu, A. Gestos, T. Lin, Robust, self-healing superamphiphobic fabrics prepared by two-step coating of fluoro-containing polymer, fluoroalkyl silane, and modified silica nanoparticles, Adv. Funct. Mater. 23 (2013) 1664–1670. https://doi.org/10.1002/adfm.201202030.

[24] J. Yang, Z. Zhang, X. Xu, X. Men, X. Zhu, X. Zhou, Superoleophobic textured aluminum surfaces, New J. Chem. 35 (2011) 2422–2426. https://doi.org/10.1039/c1nj20401g.

[25] X. Zhu, Z. Zhang, X. Xu, X. Men, J. Yang, X. Zhou, Q. Xue, Facile fabrication of a superamphiphobic surface on the copper substrate, J. Colloid Interface Sci. 367 (2012) 443–449. https://doi.org/10.1016/j.jcis.2011.10.008.

[26] X. Yao, J. Gao, Y. Song, L. Jiang, Superoleophobic Surfaces with Controllable Oil Adhesion and Their Application in Oil Transportation, Adv. Funct. Mater. 21 (2011) 4270–4276. https://doi.org/10.1002/adfm.201100775.

[27] W. Chen, A.Y. Fadeev, M.C. Hsieh, D. Öner, J. Youngblood, T.J. McCarthy, Ultrahydrophobic and ultralyophobic surfaces: some comments and examples, Langmuir. 15 (1999) 3395–3399. https://doi.org/10.1021/la990074s.

[28] K. Nakayama, E. Tsuji, Y. Aoki, H. Habazaki, Fabrication of superoleophobic hierarchical surfaces for low-surface-tension liquids, RSC Adv. 4 (2014) 30927–30933. https://doi.org/10.1039/c4ra04144e.

[29] T. Fujii, H. Sato, E. Tsuji, Y. Aoki, H. Habazaki, Important role of nanopore morphology in superoleophobic hierarchical surfaces, J. Phys. Chem. C. 116 (2012) 23308–23314. https://doi.org/10.1021/jp305078t.

[30] M. Raimondo, F. Bezzi, M. Blosi, C. Mingazzini, Method for the Treatment of Ceramic Surfaces for Bestowing Thereon a High Hydrophobicity and Oleophobicity, WO 2012/117386 A9, 2013.

[31] M. Raimondo, F. Bezzi, M. Blosi, C. Mingazzini, Method for the Treatment of Metal Surfaces for Bestowing Thereon a High Hydrophobicity and Oleophobicity, EP 2 864 522 B1, 2015.

[32] A. Chatzigrigoriou, P.N. Manoudis, I. Karapanagiotis, Fabrication of water repellent coatings using waterborne resins for the protection of the cultural heritage, in: Macromolecular Symposia, John Wiley & Sons, Ltd, 2013: pp. 158–165. https://doi.org/10.1002/masy.201300063.

[33] M. Raimondo, M. Blosi, A. Caldarelli, G. Guarini, F. Veronesi, Wetting behavior and remarkable durability of amphiphobic aluminum alloys surfaces in a wide range of environmental conditions, Chem. Eng. J. 258 (2014) 101–109. https://doi.org/10.1016/j.cej.2014.07.076.

[34] H. Liu, Y. Wang, J. Huang, Z. Chen, G. Chen, Y. Lai, Bioinspired Surfaces with Superamphiphobic Properties: Concepts, Synthesis, and Applications, Adv. Funct. Mater. 28 (2018) 1707415. https://doi.org/10.1002/adfm.201707415.

[35] UNI EN 1096-2:2012, (n.d.). http://store.uni.com/catalogo/uni-en-1096-2-2012?___store=en&josso_back_to=http%3A%2F%2Fstore.uni.com%2Fjosso-security-check.php&josso_cmd=login_optional&josso_partnerapp_host=store.uni.com&___from_store=it.

[36] T. Young, An Essay on the Cohesion of Fluids, Philosophical Transactions of the Royal Society of London. 95 (1805) 65–87. https://doi.org/10.1098/rstl.1805.0005.

[37] X. Dai, B.B. Stogin, S. Yang, T.-S. Wong, Slippery Wenzel State, ACS Nano. 9 (2015) 9260–9267. https://doi.org/10.1021/acsnano.5b04151.

[38] D. Hill, H. Attia, A.R. Barron, S. Alexander, Size and morphology dependent surface wetting based on hydrocarbon functionalized nanoparticles, J. Colloid Interface Sci. 543 (2019) 328–334. https://doi.org/10.1016/j.jcis.2019.02.058.

[39] I. Karapanagiotis, P.N. Manoudis, A. Savva, C. Panayiotou, Superhydrophobic polymer-particle composite films produced using various particle sizes, Surf. Interface Anal. 44 (2012) 870–875. https://doi.org/10.1002/sia.4930.

[40] L. Gao, T.J. McCarthy, The "lotus effect" explained: Two reasons why two length scales of topography are important, Langmuir. 22 (2006) 2966–2967. https://doi.org/10.1021/la0532149.

[41] H. Zhao, K.C. Park, K.Y. Law, Effect of surface texturing on superoleophobicity, contact angle hysteresis, and "robustness," Langmuir. 28 (2012) 14925–14934. https://doi.org/10.1021/la302765t.

[42] T. Verho, J.T. Korhonen, L. Sainiemi, V. Jokinen, C. Bower, K. Franze, S. Franssila, P. Andrew, O. Ikkala, R.H.A. Ras, Reversible switching between superhydrophobic states on a hierarchically structured surface, Proc. Natl. Acad. Sci. U.S.A. 109 (2012) 10210–10213. https://doi.org/10.1073/pnas.1204323109.

[43] A. Motta, O. Cannelli, A. Boccia, R. Zanoni, M. Raimondo, A. Caldarelli, F. Veronesi, A mechanistic explanation of the peculiar amphiphobic properties of hybrid organic-inorganic coatings by combining XPS characterization and DFT modeling, ACS Appl. Mater. Interfaces. 7 (2015). https://doi.org/10.1021/acsami.5b04376.

[44] S. Ortelli, M. Blosi, S. Albonetti, A. Vaccari, M. Dondi, A.L. Costa, TiO2 based nano-photocatalysis immobilized on cellulose substrates, J. Photochem. Photobiol. A Chem. 276 (2014) 58–64. https://doi.org/10.1016/j.jphotochem.2013.11.013.

[45] Z. Huang, W. Xu, Y. Wang, H. Wang, R. Zhang, X. Song, J. Li, One-Step Preparation of Durable Super-Hydrophobic MSR/SiO2 Coatings by Suspension Air Spraying, Micromachines. 9 (2018) 677. https://doi.org/10.3390/mi9120677.

[46] T. Ishizaki, Y. Masuda, M. Sakamoto, Corrosion resistance and durability of superhydrophobic surface formed on magnesium alloy coated with nanostructured cerium oxide film and fluoroalkylsilane molecules in corrosive NaCl aqueous solution, Langmuir. 27 (2011) 4780–4788. https://doi.org/10.1021/la2002783.

Table I. Summary of coating composition, morphology and substrates texture.

Sample code	Inorganic layer	Coating morphology	Substrate texture	Organic layer
R_SIVO	None	-	Rough	SIVO
S_SIVO	None	-	Smooth	
R_AFW	None	-	Rough	AFW
S_AFW	None	-	Smooth	
Al(ipa)*_**R**_SIVO	Al_2O_3 (ipa)	*Flower like*	Rough	SIVO
Al(w)**_**R**_SIVO	Al_2O_3 (w)			
Si_**R**_SIVO	SiO_2	*Spherical like*		
Ti _**R**_SIVO	TiO_2			
Al(ipa)_**S**_SIVO	Al_2O_3 (ipa)	*Flower like*	Smooth	SIVO
Al(w)_**S**_SIVO	Al_2O_3 (w)			
Si_**S**_SIVO	SiO_2	*Spherical like*		
Ti_**S**_SIVO	TiO_2			
Al(ipa)_**R**_AFW	Al_2O_3 (ipa)	*Flower like*	Rough	AFW
Al(w)_**R**_AFW	Al_2O_3 (w)			
Si_**R**_AFW	SiO_2	*Spherical like*		
Ti _**R**_AFW	TiO_2			
Al(ipa)_**S**_AFW	Al_2O_3 (ipa)	*Flower like*	Smooth	AFW
Al(w)_**S**_AFW	Al_2O_3 (w)			
Si_**S**_AFW	SiO_2	*Spherical like*		
Ti _**S**_AFW	TiO_2			

* ipa = isopropyl alcohol
**w = water

Table II. Contact angles against water (WCA) and n-hexadecane (CA-Hex), contact angle hysteresis (CAH) collected on rough (R) or smooth (S) aluminum alloys surfaces only coated with the organic polymers. Standard deviations are reported as errors.

Sample	WCA (°)	CA-Hex (°)	CAH (°)
R_SIVO	133 ± 5	68 ± 2	109 ± 18
S_SIVO	109 ± 3	63 ± 2	84 ± 11
R_AFW	132 ± 3	74 ± 4	113 ± 11
S_AFW	112 ± 2	65 ± 4	74 ± 4

Table III. Contact angles against water (WCA), oil (CA-Hex) and contact angle hysteresis (CAH) of hybrid coated, rough and smooth aluminum alloys substrates according to the different coating morphology. Standard deviations are reported as errors.

Sample code	WCA (°)	CA-Hex (°)	CAH	Coating morphology
Al(ipa)_**R**_SIVO	164 ± 1	111 ± 8	4 ± 2	*Flower-like*
Al(ipa)_**S**_SIVO	162 ± 5	99 ± 4	8 ± 4	
Al(ipa)_**R**_AFW	160 ± 2	114 ± 2	20 ± 9	
Al(ipa)_**S**_AFW	161 ± 3	103 ± 1	146 ± 2	
Al(w)_**R**_SIVO	166 ± 2	121 ± 11	4 ± 1	*Flower-like*
Al(w)_**S**_SIVO	167 ± 3	116 ± 3	5 ± 1	
Al(w)_**R**_AFW	163 ± 2	108 ± 1	16 ± 11	
Al(w)_**S**_AFW	161 ± 4	97 ± 4	141 ± 7	
Si_**R**_SIVO	135 ± 2	81 ± 3	73 ± 9	*Spherical-like*
Si_**S**_SIVO	120 ± 1	73 ± 2	53 ± 5	
Si_**R**_AFW	127 ± 1	76 ± 1	123 ± 10	
Si_**S**_AFW	113 ± 1	70 ± 1	85 ± 3	
Ti_**R**_SIVO	130 ± 2	83 ± 2	126 ± 5	*Spherical-like*
Ti_**S**_SIVO	120 ± 1	73 ± 1	90 ± 3	
Ti_**R**_AFW	129 ± 6	76 ± 2	129 ± 17	
Ti_**S**_AFW	113 ± 1	71 ± 1	84 ± 2	

List of figure captions

Figure 1. Flow sheets of the hybrid coatings deposition processes.

Figure 2. Schematic illustration of the multilayered coated aluminum samples.

Figure 3. FESEM images of the different inorganic layers deposited on smooth aluminum substrates: a) water-based Al_2O_3; b) alcohol-based Al_2O_3; c) SiO_2; d) TiO_2.

Figure 4. Relevance of the variables (coating morphology, substrate roughness and kind of organic layer) on the wetting behavior of hybrid coated aluminum substrates.

Figure 5. Static (WCA) and receding (RCA) contact angles against water, contact angles against oil (CA-Hex) and contact angle hysteresis (CAH) of Al_2O_3-based hybrid coatings on rough (a) and smooth (b) substrates as detected after abrasion. Standard deviations are reported as error bars.

Figure 6. Static (WCA) and receding (RCA) contact angles against water, contact angles against oil (CA-Hex) and contact angle hysteresis (CAH) of SiO_2- and TiO_2-based hybrid coatings on rough (a) and smooth (b) substrates as detected after abrasion. Standard deviations are reported as error bars.

Figure 7. Percentage depletion of contact angle against water (WCA), n-hexadecane (CA-Hex) and contact angle hysteresis (CAH), induced by the abrasion test on *flower-like* and *spherical-like* coatings.

Figure 8. FESEM micrographs collected after abrasion testing on samples Al_2O_3(ipa)_R_SIVO (a, b) and Si_R_SIVO (c, d).

Figure 9. Trends of contact angle against water (WCA) of amphiphobic surfaces soaked into saline, acidic and basic solutions. Standard deviations are reported as error bars.

Figures

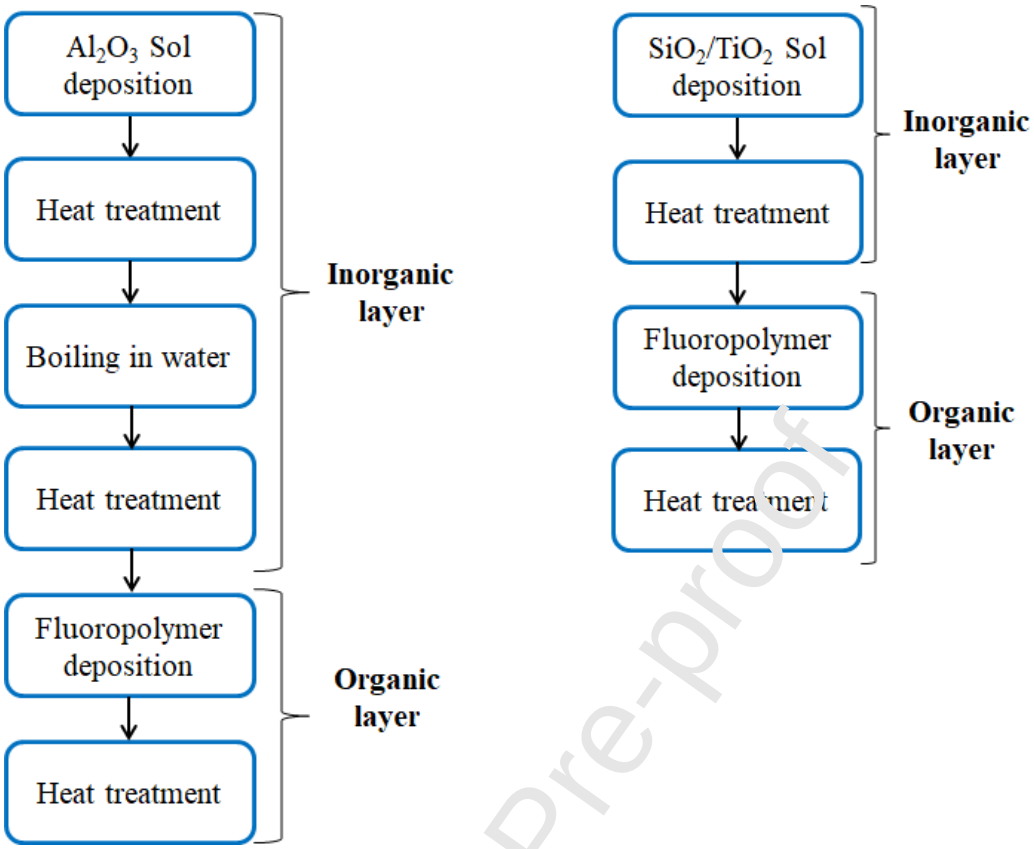

1

2

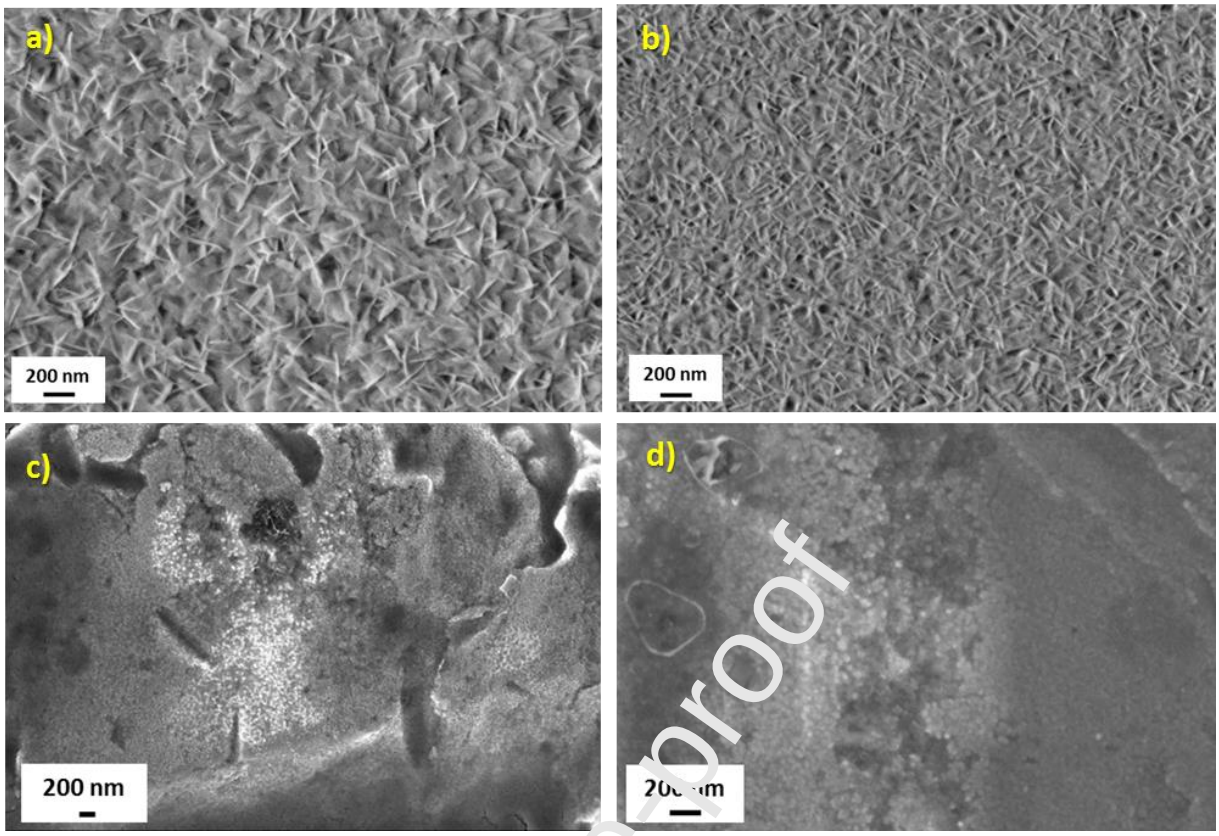

3

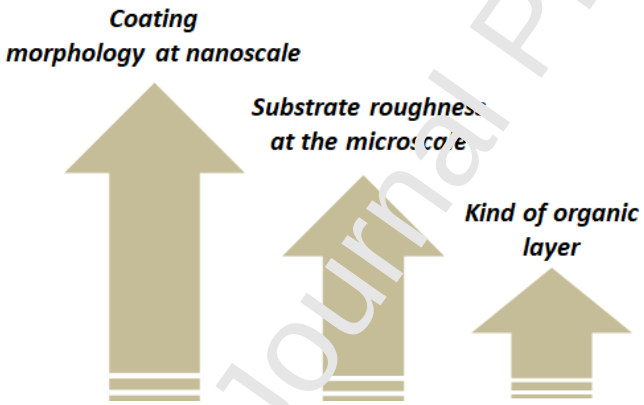

4

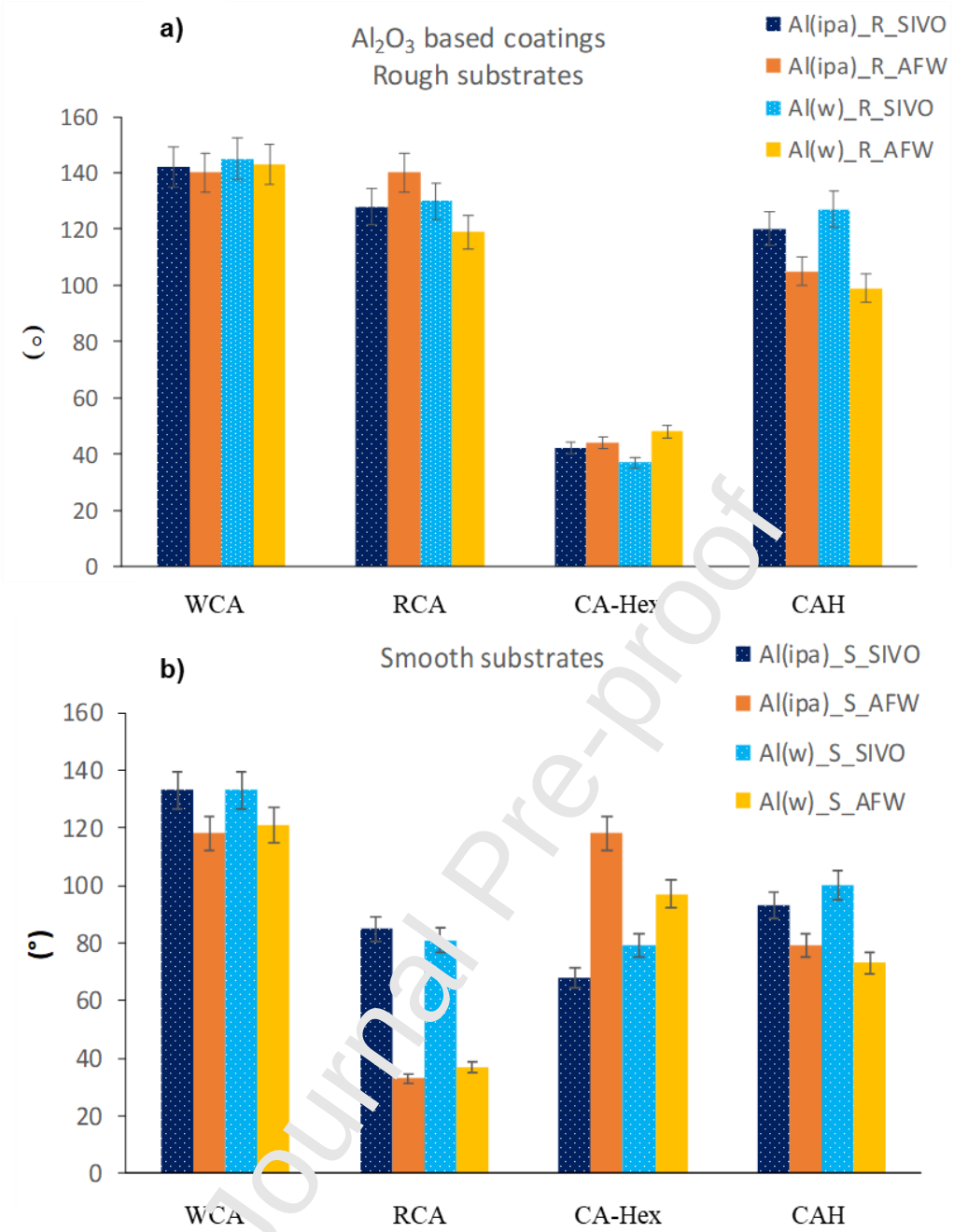

5

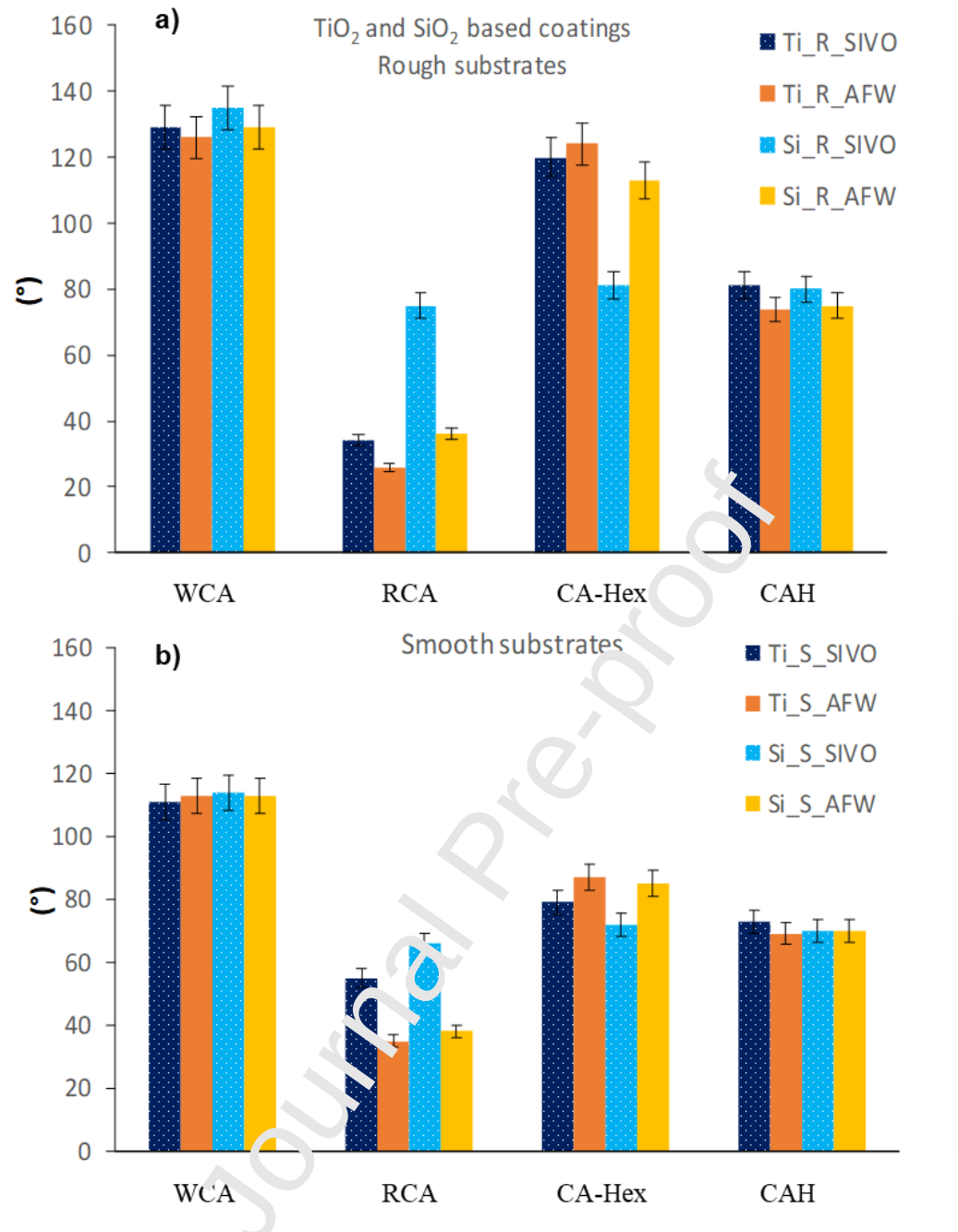
a)
TiO2 and SiO2 based coatings
Rough substrates
Ti_R_SIVO
Ti_R_AFW
Si_R_SIVO
Si_R_AFW
(°)
WCA
RCA
CA-Hex
CAH
b)
Smooth substrates
Ti_S_SIVO
Ti_S_AFW
Si_S_SIVO
Si_S_AFW
(°)
WCA
RCA
CA-Hex
CAH

6

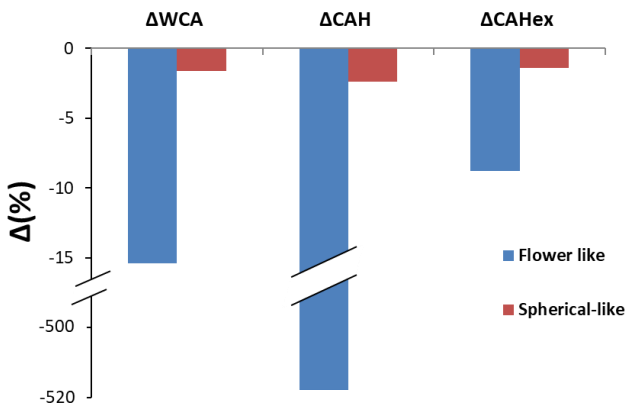
ΔWCA
ΔCAH
ΔCAHex
Δ(%)
Flower like
Spherical-like

7

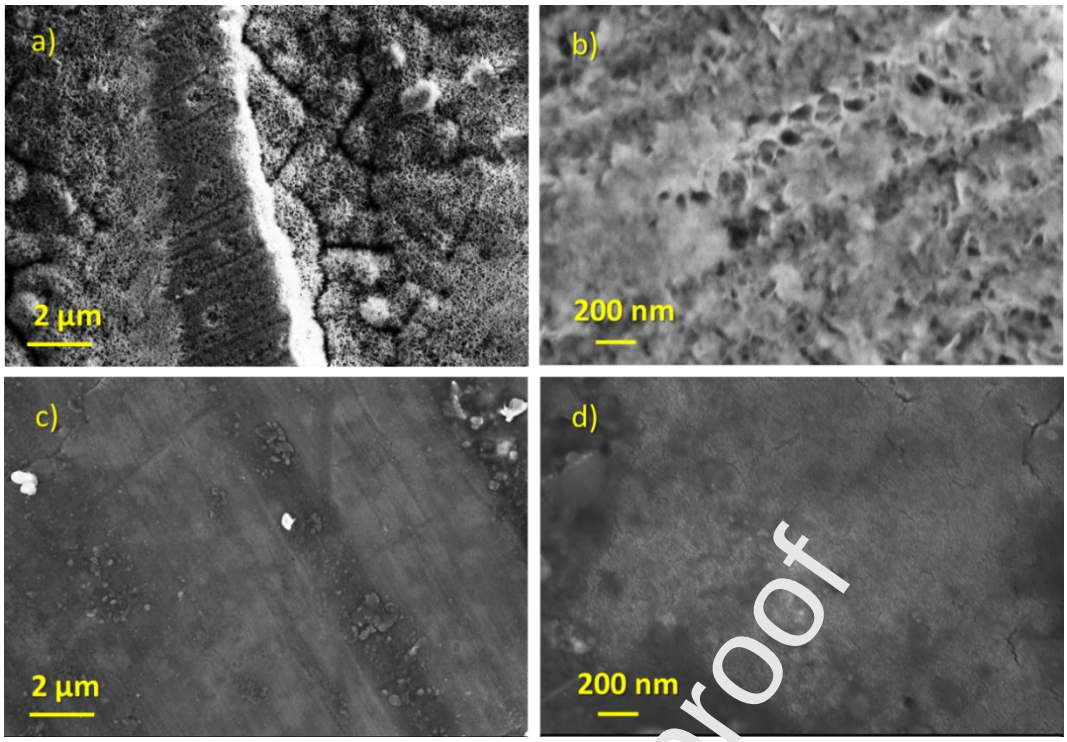

8

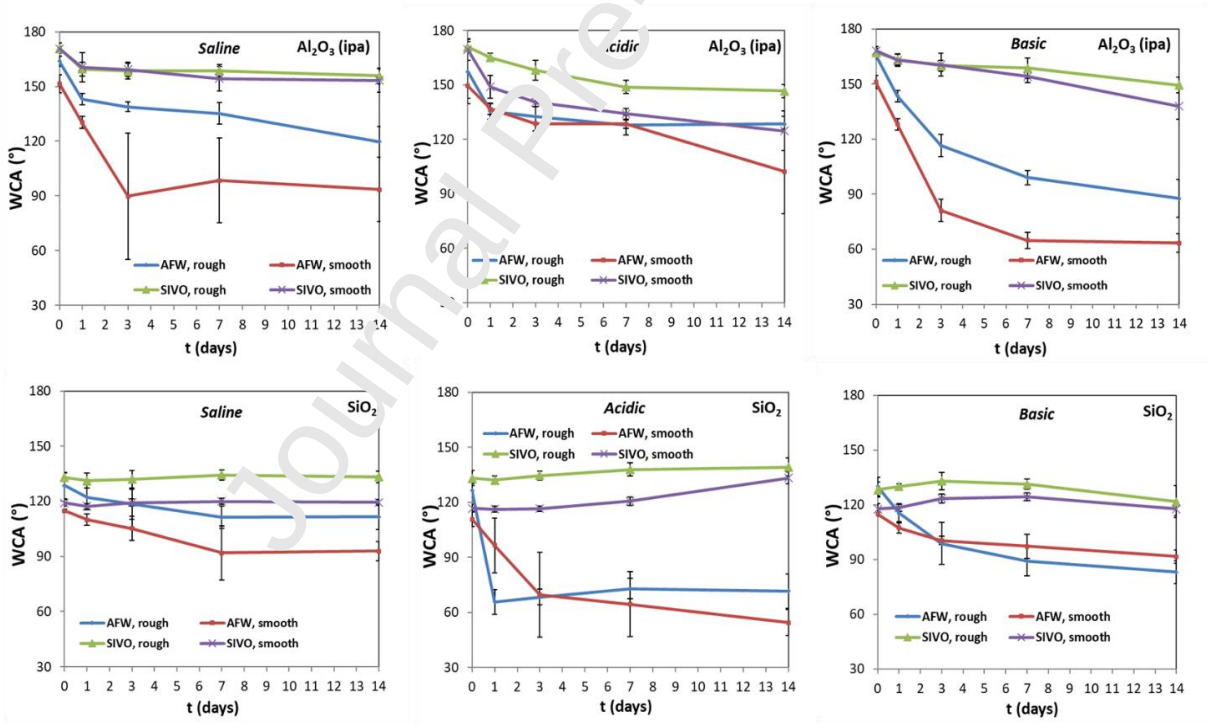

9

Graphical Abstract

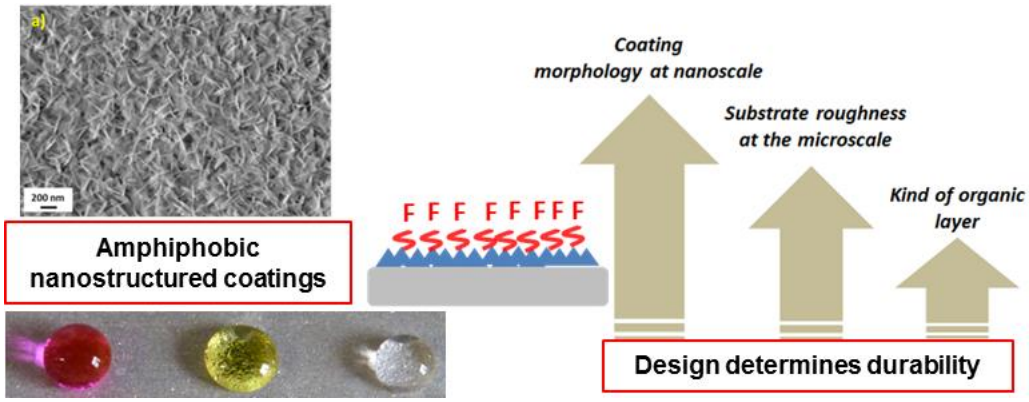

Highlights

~~The paper focus on the design and fabrication of amphiphobic surfaces for a better understanding of the role played by the substrate texture and processing variables by a step-by-step approach~~

A step by step exploration for the design of amphiphobic coatings was undertaken

~~Coating processes were applied to Al alloys with different surface roughness by deposition of nanostructured ceramic oxide (Al_2O_3, SiO_2 and TiO_2) and fluoro-polymers (fluoroalkylsilane or acrylic resin)~~

Different nanostructured ceramic oxide and fluoro-polymers were applied on Al alloys

~~The relevance of the substrate/coating variables to maximize both static and dynamic repellence against liquids follows the order: morphology of the inorganic layer (*flower-* or *spherical like*) > substrate roughness at microscale > nature of organic fluoropolymer~~

The relevance of morphology, surface roughness and layers composition was highlighted

~~Most coated surfaces showed a good ability to withstand severe environments. When occurring, the different response stems from the different composition of the inorganic layers and not from the overall morphology of the coatings~~

Amphiphobic surfaces showed a good ability to withstand severe environments

~~Overall, the perspectives for the application of hybrid coated Al are related in a complex way to many variables influencing the products final performances which, in turn, could stay unchanged or vary in a more or less wide range depending on environments and exposure conditions~~

The development of hybrid coated Al are related in a complex way to many variables